

Infra-red study of hydrogen bonding in amine-crosslinked epoxies

V. Bellenger and J. Verdu

ENSAM, 151 Bd de l'Hôpital, 75013 Paris, France

and J. Francillette and P. Hoarau

ETCA, 16 bis Av. Prieur de la Côte d'Or, 94114 Arcueil, France

and E. Morel

IRCHA, BP 1, 91710 Vert le Petit, France

(Received 12 June 1986; revised 12 October 1986; accepted 17 October 1986)

Comparison of infra-red spectra of various epoxide-amine networks in the hydroxyl stretching region ($3600\text{--}3200\text{ cm}^{-1}$) reveals the existence of at least three components. The first one, 'M', centred at $3400\text{--}3420\text{ cm}^{-1}$, can be attributed to intermolecular ($\text{OH}\cdots\text{OH}$) bonding. The second one, 'L', a diffuse band in the low-wavenumber part of the spectrum, can be attributed to a ($\text{OH}\cdots\text{N}$) chelate. The third one, 'H', a sharp shoulder at 3550 cm^{-1} , whose intensity increases with temperature, can be attributed to intramolecular dimeric association of two hydroxyls linked to the same nitrogen atom. The variations of their relative importance with the amine structure and the crosslink density are discussed in terms of steric configurations around the sec-alcohol- α -aminomethylene bond and amine nucleophilicity.

(Keywords: infra-red spectra; hydrogen bonding; epoxies)

INTRODUCTION

Although infra-red (i.r.) spectrophotometry is generally considered as a good tool for hydrogen-bonding studies¹, its application to amine-crosslinked epoxies is not very easy, for at least two reasons.

The first one is common to all densely crosslinked systems: they are insoluble, so that it is generally difficult to obtain samples of well defined structure because their complete curing needs high-temperature treatments which can induce side reactions, and we lack precise methods for determination of their final state. I.r. data on hydroxyl bands, for instance, can be used to follow the course of crosslinking in a given system, as shown many years ago², but it is difficult to compare one system with another, because sample thicknesses are not always known and the internal standard bands sometimes used are poorly defined with the common sampling methods (KBr pellets, capillary films, etc.).

The second reason is specific to amine-crosslinked epoxies and is related to the probable coexistence of many hydrogen-bonded species (*Figure 1*). The overlapping of their absorption bands leads to a broad band displaying practically no fine structure except, in certain cases, a small shoulder² near 3550 cm^{-1} . Comparative studies of model compounds seem to show that all hydroxyls are bonded in the condensed state, and that 'intermolecular' bonds largely predominate³. In contrast, indirect observations on water absorption and comparison of the hydroxyl stretching band area seem to be explainable only by the occurrence of a $\text{OH}\cdots\text{N}$ intrasegmental bond whose importance depends sharply on the amine nucleophilicity⁴. The equilibrium between various

hydrogen-bonded species can be easily shifted by a change of temperature, and quantitative data on this phenomenon can give interesting information on the nature of hydrogen bonds. Some variable temperature measurements were made in the case of epoxies^{5,6}. They revealed the persistence of hydrogen-bonded species and the apparent total absence of unbonded hydroxyls up to 200°C .

Since we developed a method for the preparation of thin films allowing precise transmittance measurements on networks of relatively well defined structure⁷, it seemed interesting to make a detailed comparative study of the hydroxyl band shape for systems differing by the following structural parameters: electron density on nitrogen atom, steric hindrance around the tertiary amine, crosslink density and epoxide/amine molar ratio.

EXPERIMENTAL

Epoxides and amines

The structure and codes of epoxides and amines under study are presented in *Figure 2*.

In the case of DGEBA and DGEBF, the degree of polymerization j was determined from chemical titration of epoxide groups. The hydroxyls present in the oligomers were taken into account in the calculation of OH concentration in networks:

$$[\text{OH}] = \frac{4 + 2j}{2M_e + M_a}$$

where M_e and M_a are respectively the molar mass of the diepoxide and of the diamine.

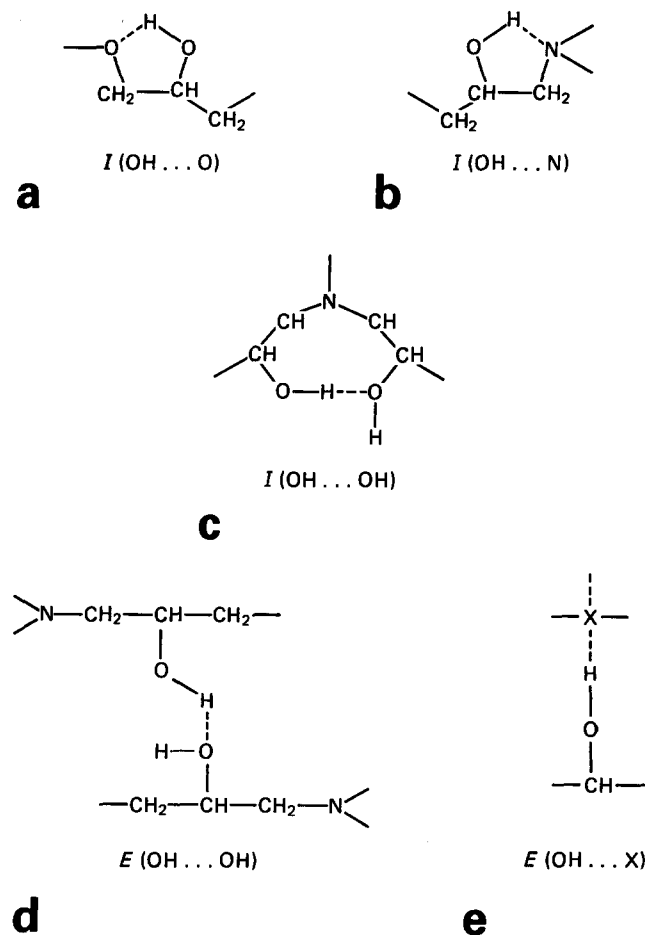


Figure 1 Some possible types of intramolecular, $I(\square)$, or intermolecular, $E(\square)$, hydrogen bonds in epoxide-amine networks (X = electronegative atom)

In the case of TGMDA, whose epoxide concentration is 84% of its theoretical value (9.48 mol kg^{-1}), the experimental value of epoxide index was taken into account for the determination of the stoichiometric amine concentration. The hydroxyls present in the uncrosslinked TGMDA were neglected in the calculation so that:

$$[\text{OH}] = \frac{4 \times 0.84}{M_e + 0.84M_a}$$

G.p.c. analysis ($2 \times 100 \text{ \AA}$ plus $1 \times 500 \text{ \AA}$, refractometric detection) revealed the presence of a single peak for all amines under study. Only aniline was distilled before use. For the monoepoxide, (PGE), a small amount of dimer was found.

Films

Solutions of amine and epoxide in tetrahydrofuran (THF), methanol or acetone, depending on the system studied, were mixed and ultrasonically homogenized. Then, they were cast on clean mercury surfaces and heated for 1 h at $70\text{--}120^\circ\text{C}$ depending on the system under study. A second curing stage at $130\text{--}190^\circ\text{C}$ allowed curing to be achieved, except for TGMDA systems, in which a latter stage at 250°C in vacuum is needed. The extent of cure is characterized by classical methods: T_g and residual cure exotherm by d.s.c., residual epoxide groups by i.r. at 910 cm^{-1} . For each system, the maximum (asymptotic)

value of the glass transition temperature ($T_{g,\infty}$) was previously determined from d.s.c. experiments. Then, the temperature and duration of cure treatments were optimized in order to obtain:

$$T_{g,\infty} - 30 \text{ K} \leq T_g \leq T_{g,\infty}$$

and to avoid the formation of oxidation products (carbonyl and amide groups⁷) in noticeable concentrations. In these conditions, the solvent was completely eliminated as confirmed by i.r. and gravimetric measurements.

The volume and concentration of the starting solutions were chosen in order to obtain films of $10\text{--}200 \mu\text{m}$ thickness. Only films of $20\text{--}40 \mu\text{m}$ were used for the comparative study.

Model compounds

The preparation and characterization of PGE-diamine adducts will be reported elsewhere.

Differential scanning calorimetry

D.s.c. traces were obtained with a Perkin-Elmer DSC 2 apparatus on $2\text{--}5 \text{ mg}$ samples at 20 K min^{-1} scanning rate. T_g was determined as the inflection point of the thermogram.

Infra-red spectrophotometry

The films were used in the dry state. We used two apparatus: Perkin-Elmer 198 and 580. The peak at 1885 cm^{-1} (*p*-phenylene) was chosen as internal standard. Measurements on many films of various thicknesses allowed us to determine its extinction coefficient E_S :

$$A_S = E_S d$$

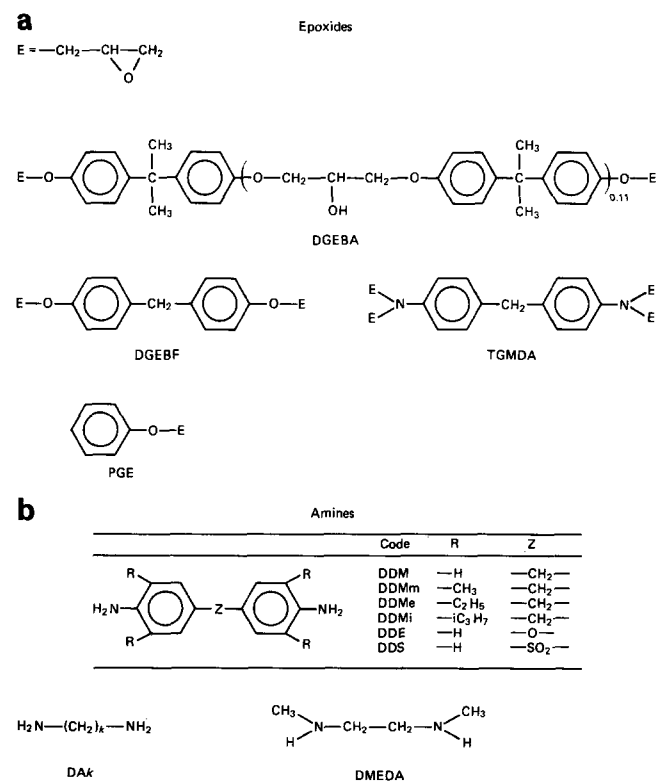


Figure 2 Formulae and codes for epoxides and amines under study

where A_s is the absorbance measured from a tangent baseline and d the thickness in centimetres.

The E_s values varied systematically by 10–15% from one apparatus to another. This is probably due to differences in the beam convergence at the sample. The variations were taken into account in the calculations.

The absorbance values at various wavenumbers within the hydroxyl band were taken from a tangent baseline. For the maximum absorbance A_M , we determined:

$$I(\text{OH}) = \frac{A_M}{A_s} \times E_s$$

the absorbance per thickness unit expressed in cm^{-1} .

Some values of $T_{g,\infty}$ and E_s for the systems under study are presented in Table 1.

Variable temperature measurements

We used a Perkin-Elmer 580 equipped with its data station and a variable temperature accessory. Measurements were made at 27, 80, 160, 180, 200, 225 and 250°C after thermal equilibrium was reached. More experimental details will be given elsewhere. Results will be reported only on the DGEBA-DDM almost completely cured system.

RESULTS

Comparison of stoichiometric networks differing in the diepoxide structure

Some spectra in the hydroxyl stretching range are presented in Figures 3 (DGEBA systems), 4 (DGEBF systems) and 5 (TGMDA systems). The following observations can be made:

(a) In all cases, the absorption maximum lies at $3410 \pm 10 \text{ cm}^{-1}$.

(b) The band shape depends essentially on the diamine structure: the DGEBA systems display the same features as their DGEBF or TGMDA homologues.

Table 1 Characteristics of networks under study: f , hardener fraction in percentage of the stoichiometric concentration; aniline content in per cent; E_s , absorbance per thickness unit of the internal standard band; T_g , glass transition temperature of almost completely cured samples; $[\text{OH}]$, theoretical hydroxyl concentration

Systems	f (%)	Aniline (%)	E_s (cm^{-1})	T_g (K)	$[\text{OH}]$ (mol kg^{-1})
DGEBA-DDM	100	0	23	451	4.50
DGEBA-DDE	100	0	20	446	4.49
DGEBA-DDS	100	0	25	483	4.27
DGEBF-DDM	100	0	21	430	4.87
DGEBF-DDE	100	0	18	425	4.82
DGEBF-DDS	100	0	25.6	456	4.59
TGMDA-DDM	100	0	19.5	505	5.71
TGMDA-DDE	100	0	20.6	497	5.70
DGEBA-DA2	100	0	11.5	395	5.27
DGEBA-DA4	100	0	11.5	393	5.10
DGEBA-DA12	100	0	11.5	361	4.49
DGEBA-DDMm	100	0	15	428	4.25
DGEBA-DDMe	100	0	12.5	420	4.02
DGEBA-DDMi	100	0	12	406	3.82
DGEBA-DDM	50	0	—	≤ 320	2.65
DGEBA-DDM	65	0	—	353	3.25
DGEBA-DDM	75	0	—	375	3.62
DGEBA-DDM	85	0	—	401	3.99
DGEBA-DDM	67	33	—	401	4.53
DGEBA-DDM	50	50	—	393	4.53
DGEBA-DDM	33	67	—	382	4.54

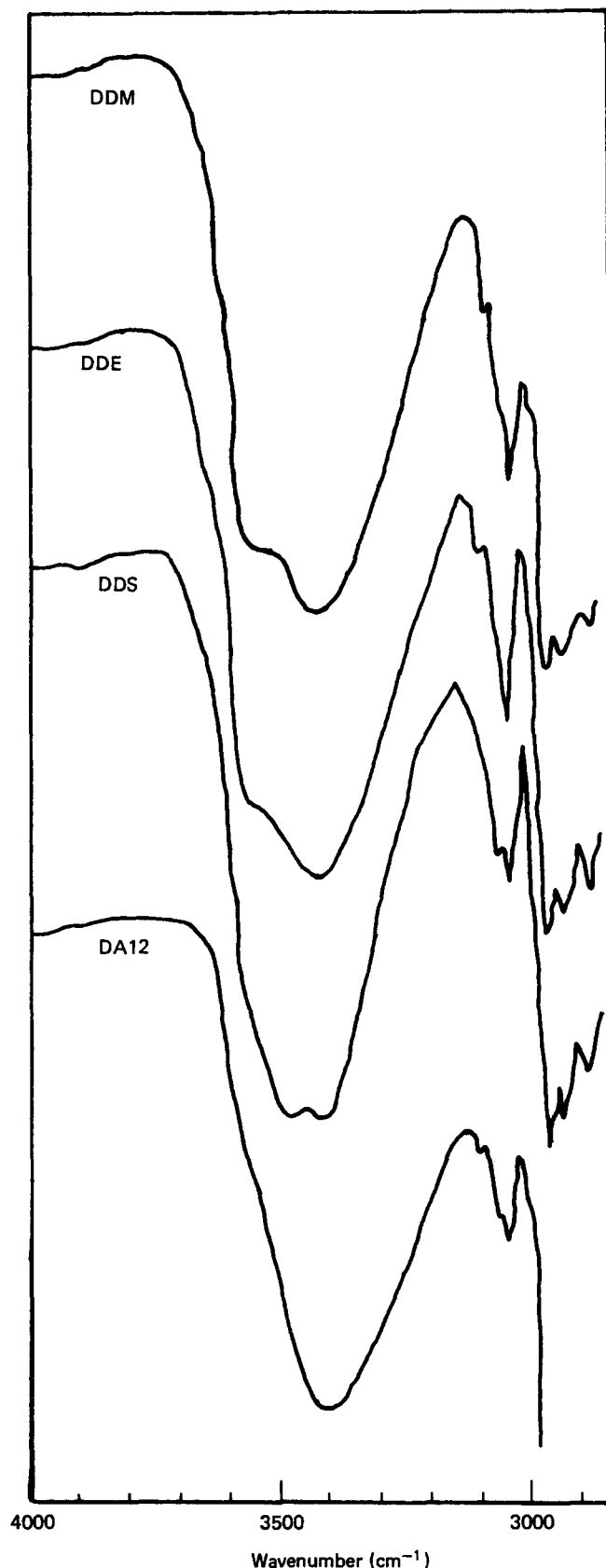


Figure 3 I.r. spectra in the hydroxyl region of DGEBA systems

(c) No fine structure can be observed in systems crosslinked with aliphatic diamines (DAk), whose band tails are bathochromically shifted relative to those of homologous systems crosslinked by aromatic amines.

(d) All the systems based on aromatic diamines display 'fine structure': a sharp shoulder appears at $\approx 3550 \text{ cm}^{-1}$.

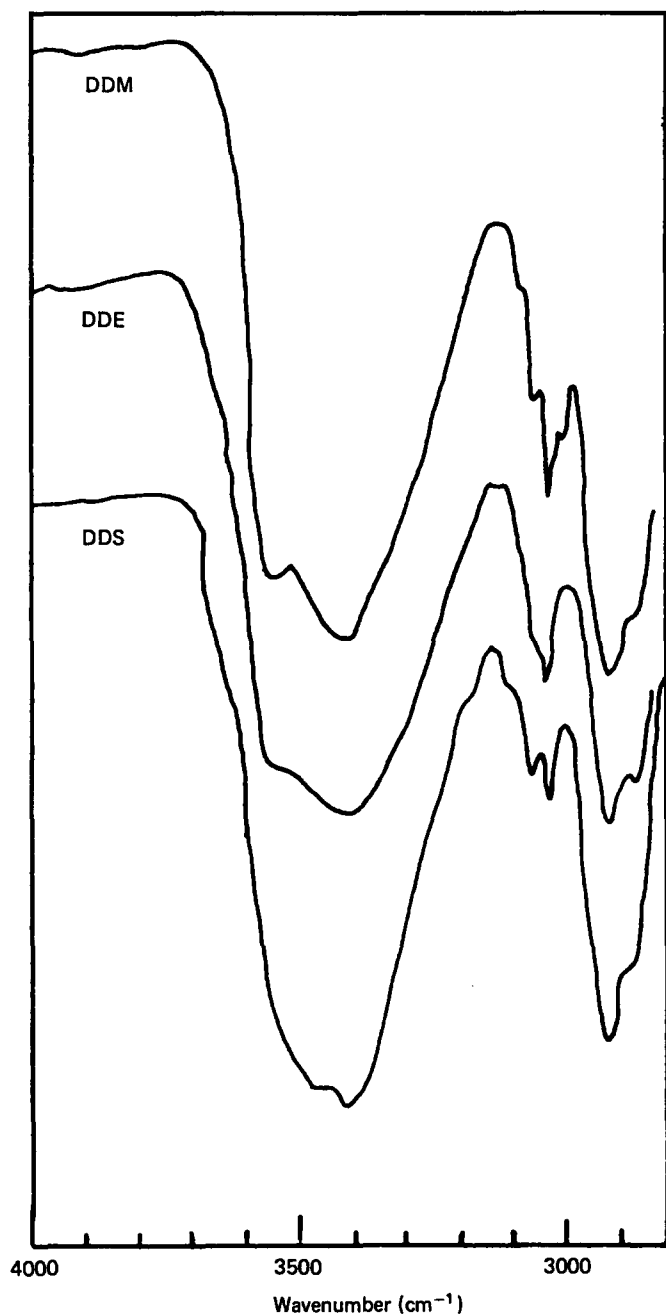


Figure 4 I.r. spectra in the hydroxyl region of DGEBF systems

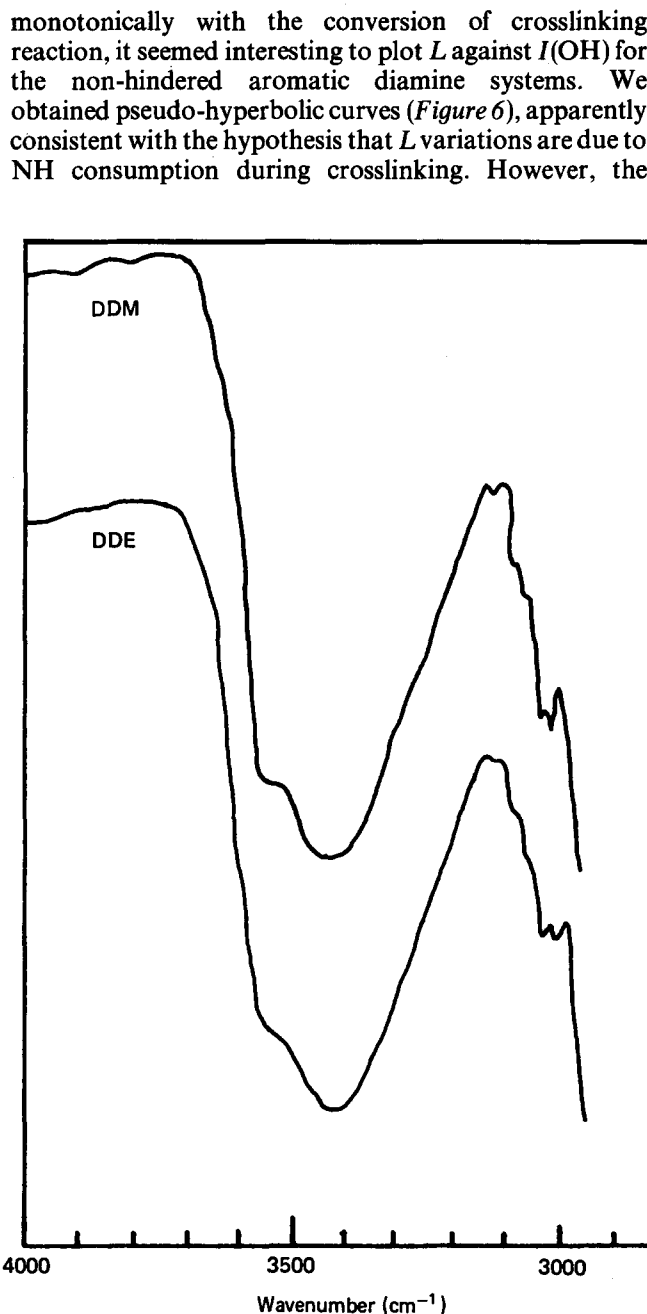


Figure 5 I.r. spectra in the hydroxyl region of TGMDA systems

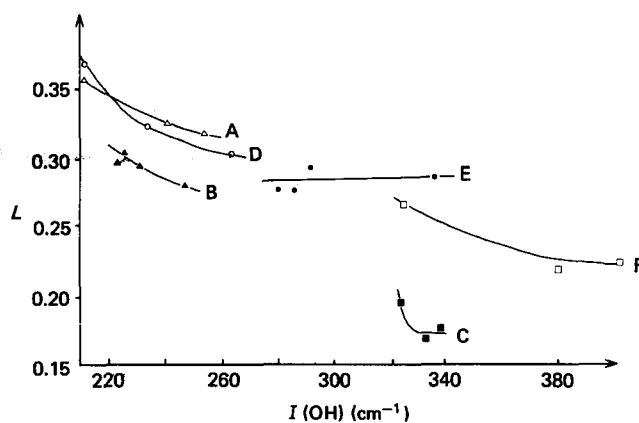
Its intensity decreases with the bulkiness of *ortho* substituents in the series DDM—DDMm—DDMe—DDMi.

(e) In the case of DDS systems, whose overall half bandwidth is noticeably lower than the preceding ones, a supplementary, relatively wide, component can be observed at $\approx 3460\text{ cm}^{-1}$.

In order to quantify the observed differences, we determined the absorbance at the maximum absorption (A_M), the absorbance at the shoulder ($\approx 3550\text{ cm}^{-1}$) (A_H) and the absorbance at an arbitrarily chosen wavenumber, 3260 cm^{-1} on the right tail of the band (A_L). Then, we determined $I(\text{OH}) = A_M/d$, $E(\text{OH}) = I(\text{OH})/[\text{OH}]$, $H = A_H/A_M$ and $L = A_L/A_M$.

The significance of L values could be questioned since NH residual groups absorb near 3200 cm^{-1} . Since we examined many samples differing slightly in their cure treatment, and since $I(\text{OH})$ increases almost

monotonically with the conversion of crosslinking reaction, it seemed interesting to plot L against $I(\text{OH})$ for the non-hindered aromatic diamine systems. We obtained pseudo-hyperbolic curves (Figure 6), apparently consistent with the hypothesis that L variations are due to NH consumption during crosslinking. However, the

Figure 6 Dependence of L on $I(\text{OH})$ for DGEBA–DDE (curve A), DGEBA–DDM (curve B), DGEBA–DDS (curve C), DGEBF–DDE (curve D), DGEBF–DDM (curve E) and DGEBF–DDS (curve F)

asymptotic values of L differ noticeably from one system to another.

Typical values of $I(\text{OH})$, $E(\text{OH})$, L and H for almost completely cured samples are presented in Table 2. It can be observed that for the non-sterically hindered amines, L seems to be correlated with the amine reactivity in crosslinking: $\text{DAk} > \text{DDE} > \text{DDM} > \text{DDS}$. It can be seen

Table 2 Maximum absorbance per thickness unit, $I(\text{OH})$, apparent molar absorptivity, $E(\text{OH})$, and H and L ratios (see text) for various stoichiometric systems almost completely cured

System	$I(\text{OH})$ (cm^{-1})	$E(\text{OH})$ ($\text{kg mol}^{-1} \text{cm}^{-1}$)	H	L
DGEBA-DDM	247	55	0.75	0.28
DGEBA-DDA	254	57	0.71	0.32
DGEBA-DDS	337	79	0.68	0.17
DGEBF-DDM	292	60	0.75	0.29
DGEBF-DDE	263	55	0.76	0.30
DGEBF-DDS	404	88	0.65	0.22
TGMDA-DDM	297	52	0.69	0.32
TGMDA-DDE	277	49	0.67	0.30
DGEBA-DA2	151	29	0.46	0.38
DGEBA-DA4	155	30	0.52	0.33
DGEBA-DA12	155	35	0.36	0.41
DGEBA-DDMm	250	59	0.57	0.36
DGEBA-DDMe	212	53	0.49	0.43
DGEBA-DDMi	170	45	0.52	0.41

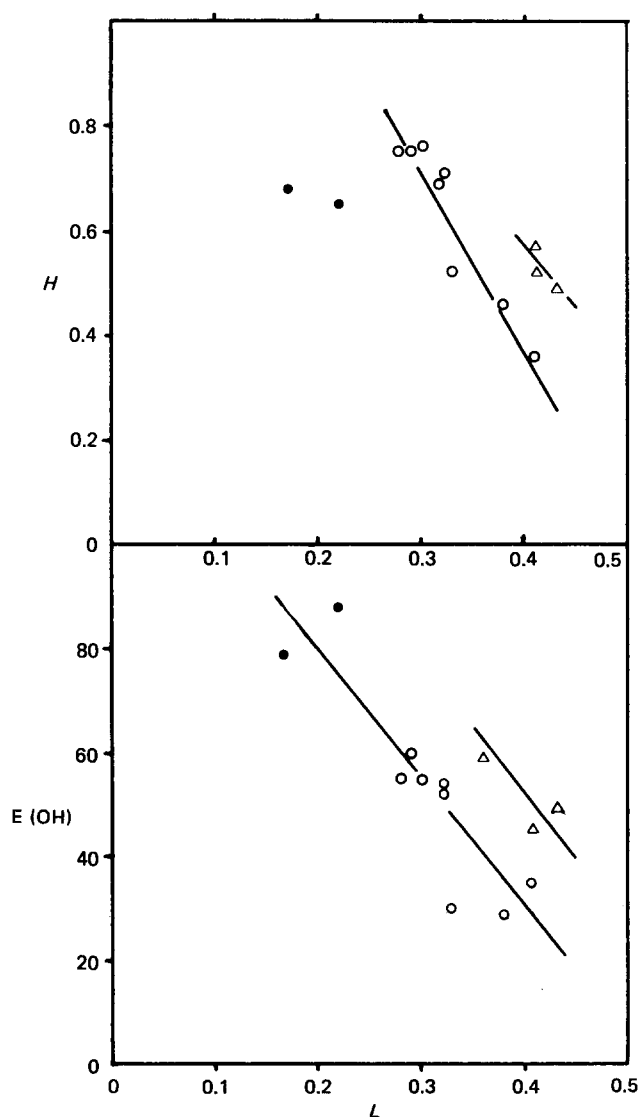


Figure 7 Dependence of H and $E(\text{OH})$ on L for almost completely cured samples: ●, DOS; △, alkyl-substituted DDM; ○, other systems

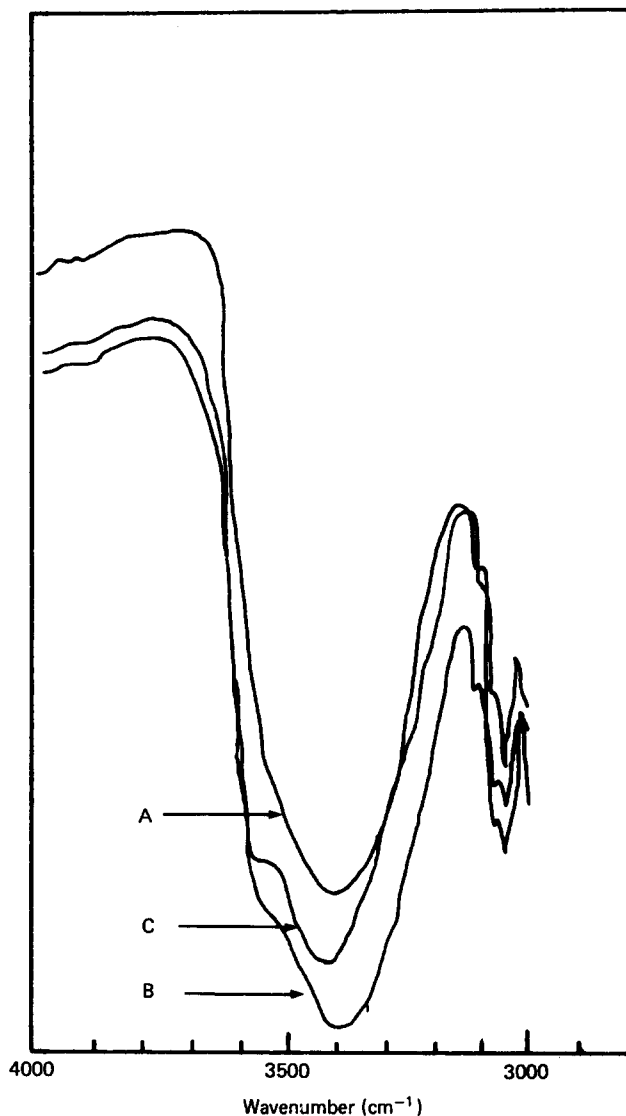


Figure 8 I.r. spectra in the hydroxyl region of some DGEBA-DDM systems: curve A, DDM 50%; curve B, aniline 67%; curve C, DDM 100%

in Figure 7 that $E(\text{OH})$ and H decrease more or less regularly with L .

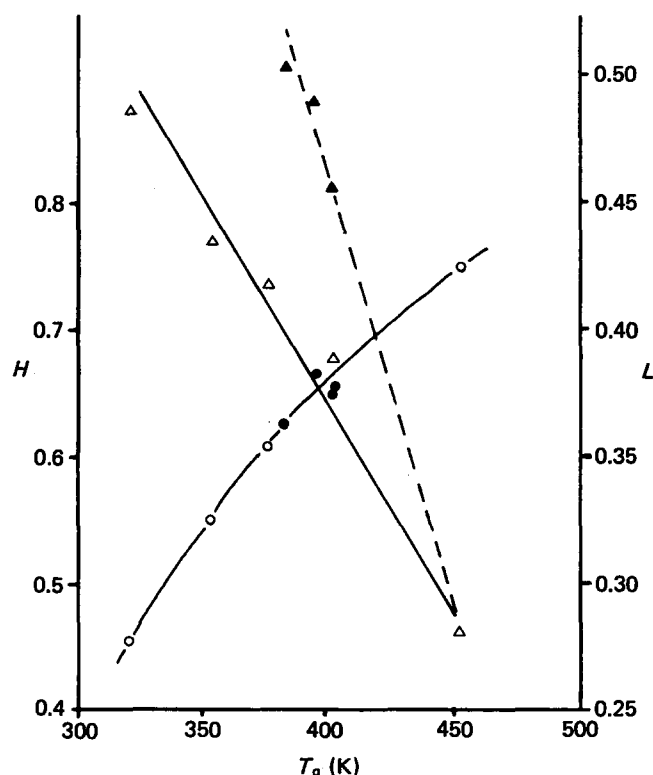
Influence of the crosslink density in DGEBA-DDM systems

We studied two series of samples. In the first one, DDM was in the concentration of respectively 50, 65, 75 and 85% of the stoichiometric value. The cure conditions were 3 h at 160°C. In the second one, DDM was in the concentration of respectively 33, 50 and 67% of the stoichiometric value, but complementary quantities of aniline were added in order to complete the epoxide consumption and to obtain overall hydroxyl concentrations near to those existing in the DGEBA-DDM stoichiometric system. The cure conditions were 1 h at 70°C, 1 h at 170°C and 1 h at 190°C.

Since the final stage of the cure is made at a temperature noticeably higher than the final glass transition temperature ($T_{g,\infty} \leq 401 \text{ K}$), it can be reasonably considered that the epoxide-amine addition is complete in both series. Some spectra are presented in Figure 8. The theoretical hydroxyl concentrations $[\text{OH}]$ and crosslink densities n , the glass transition temperatures T_g and the L and H ratios are reported in Table 3. It can be seen in Figure 9 that H increases and L decreases with T_g .

Table 3 Crosslink density, H and L values for DGEBA-DDM and DGEBA-DDM-aniline systems

DDM (%)	Aniline (%)	n (mol kg ⁻¹)	H	L
50	0	0	0.457	0.485
65	0	0	0.551	0.435
75	0	0.56	0.608	0.418
85	0	1.10	0.654	0.390
67	33	1.42	0.648	0.456
50	50	1.08	0.664	0.490
33	67	0.71	0.623	0.503
100	0	2.13	0.750	0.280

**Figure 9** Dependence of H (circles) and L (triangles) on the glass transition temperature for DGEBA-DDM systems: open symbols, DGEBA-DDM; closed symbols, DGEBA-DDM-aniline systems

Plotting H and L against crosslink density, we should obtain the same type of curve.

In this case, the internal standard peak at 1885 cm^{-1} was not studied, so that we do not know precise values of $I(\text{OH})$. However, from a single determination of the film thickness, it can be estimated that $I(\text{OH})$ varies almost proportionally with $[\text{OH}]$: $E(\text{OH}) \approx 55$ to $63\text{ kg mol}^{-1}\text{ cm}^{-1}$. Thus, in this case, the 'H' species seems to be formed mainly at the expense of the 'L' one.

Study of unreacted oligomeric diepoxide and model compounds

The spectra of unreacted DGEBA (0.11), PGE-DA6 and PGE-DMEDA adduct are presented in Figure 10. In the case of DGEBA (0.11) a single, relatively sharp, component is centred at $3500\text{--}3510\text{ cm}^{-1}$. The spectra of PGE-aliphatic diamine adducts are very similar to those of DGEBA-aliphatic diamine networks. They are characterized by the absence of the 'H' species and a high L value. For PGE-DA6, $H = 0.427$, $L = 0.582$; for PGE-DMEDA, $H = 0.470$, $L = 0.579$.

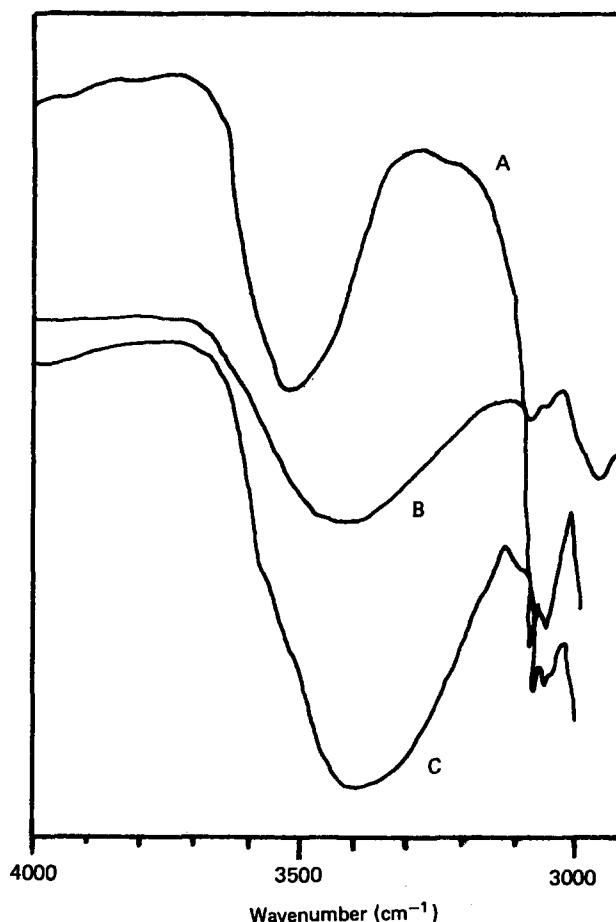
No significant difference appears between the primary (DA6) and secondary (DMEDA) diamine.

Influence of temperature on the spectrum of DGEBA-DDM

Spectra taken at various temperatures ranging from 25 to 250°C are shown in Figure 11. As T increases, the main component decreases in intensity and shifts towards high wavenumbers. However, the intensity of the 'H' component increases.

DISCUSSION

The characteristics of the 'M' band ($\bar{\nu}_{\text{max}} = 3410 \pm 10\text{ cm}^{-1}$, $E_{\text{max}} = 30\text{--}70\text{ kg mol cm}^{-1}$) are close to those of low-molecular-weight alcohols in which polymeric associates predominate. The effects of a temperature increase (Figure 11) are qualitatively the same as in simple models such as, for instance, benzyl alcohol⁸. They can be well explained by a disruption of hydrogen bridges and a shortening of associates¹. Thus, 'M' is obviously the intermolecularly $E(\text{OH} \dots \text{OH})$ bonded hydroxyl band. The only system in which its maximum is noticeably shifted is the unreacted DGEBA ($\bar{\nu}_{\text{max}} = 3500\text{--}3510\text{ cm}^{-1}$). We also note, in this case, a considerable reduction of bandwidth $\Delta\bar{\nu}$ relative to networks (Figure 10). Such a shift, associated with such a reduction of $\Delta\bar{\nu}$, is characteristic of intermolecular bonds⁹. Moreover, it was found that in solid-state organic compounds, $\bar{\nu}_{\text{max}}$ increases with the hydrogen bond distance¹⁰. Thus, the peculiarity of unreacted DGEBA can be well explained by its low hydroxyl concentration (0.3 mol kg^{-1} against $\geq 4\text{ mol kg}^{-1}$ in stoichiometric networks), which results in a higher average $\text{OH} \dots \text{OH}$ distance.

**Figure 10** I.r. spectra in the hydroxyl region of unreacted DGEBA (curve A), PGE-DMEDA adduct (curve B) and PGE-DA6 adduct (curve C)

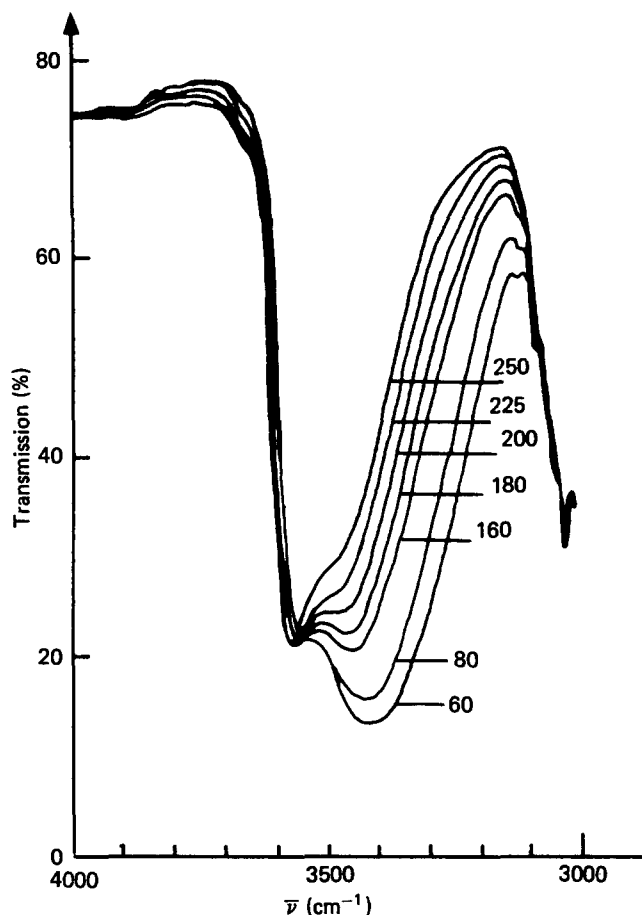


Figure 11 I.r. spectra in the hydroxyl region of a DGEBA-DDM stoichiometric sample at various temperatures. The numbers on the figure indicate the temperature (°C)

The characteristics of the shoulder 'H' (relatively sharp band, $\bar{\nu}_{\max} \approx 3550 \text{ cm}^{-1}$) seem to be related to a dimeric $[\text{OH} \dots \text{OH}]$ association^{1,11}. The fact that its intensity increases with temperature until 250°C (Figure 11) and that it does not appear in similar experiments on low-molecular-weight alcohols, as reviewed by Pimentel and McClellan¹, is clearly in favour of an intramolecularly $I(\text{OH} \dots \text{OH})$ bonded species (Figure 1c).

Two alternative explanations could be offered for the opposite variations of $E(\text{OH})$ and L .

(a) These variations are due to changes in the length distribution of polymeric associates and/or packing density.

(b) There is a peculiar species 'L' characterized by a diffuse band in the low-wavenumber range.

Since we observed that L is related to the amine reactivity in crosslinking, and since Eichler and Mleziva determined the electron density q on nitrogen by quantum-mechanical calculations for aromatic diamines¹², it seemed interesting to try to correlate L with q for DDS, DDM and DDE systems. The almost linear relationship (Figure 12) indicates that the amine seems to be directly involved in hydrogen bonding.

Since, in the DGEBA-DDM series, L decreases with the overall hydroxyl concentration, which is contradictory of the first hypothesis, and since L does not decrease with the amine shielding (DDM < DDMi), it can be deduced that 'L' is an intrasegmental $I(\text{OH} \dots \text{N})$ bonded species. The literature data on model compounds are in good agreement with this hypothesis: chelates are

characterized by diffuse bands in the low-wavenumber range, sometimes at $\bar{\nu} < 3000 \text{ cm}^{-1}$.^{1,11} Let us consider the two sec-alcohols connected with a given N atom and compare $E(\text{OH})$ values for DGEBA-DDS and DGEBA-DAk systems: $E(\text{OH}) \approx 80 \text{ kg mol}^{-1} \text{ cm}^{-1}$ (DDS) against $\approx 30 \text{ kg mol}^{-1} \text{ cm}^{-1}$ (DAk). Since the specific weight is $\approx 1.25 \text{ g cm}^{-3}$ for DGEBA-DDS and $\approx 1.1 \text{ g cm}^{-3}$ for DGEBA-DAk, we obtain $\epsilon(\text{OH}) \approx 63 \text{ l mol}^{-1} \text{ cm}^{-1}$ for DGEBA-DDS and $\approx 27 \text{ l mol}^{-1} \text{ cm}^{-1}$ for DGEBA-DAk. This is consistent with the hypothesis that, in DGEBA-DDS, both hydroxyls connected with a given N atom are O bonded, whereas in DGEBA-DAk, approximately one hydroxyl is O bonded and the other N bonded.

It is not surprising to find the highest L values in model compounds made from aliphatic diamines. In contrast, the fact that PGE-DMEDA displayed the same characteristics as PGE-DA6 adduct is somewhat unexpected. As a matter of fact, in the former system, there is only one sec-alcohol connected to a nitrogen atom of high electron density, so that all hydroxyls could be N bonded. This result can be explained if, in a $-\text{CH}(\text{OH})-\text{CH}_2-\text{N}<$ segment, only one stereoisomer is able to form the chelate, the other participating in $(\text{OH} \dots \text{OH})$ bonds.

The fraction of $I(\text{OH} \dots \text{N})$ bonded stereoisomers depends on the competitiveness of the various other hydrogen acceptors present, e.g. on q , but also on the segmental mobility as shown by L variations in the DGEBA-DDM series. This latter result can also be interpreted in terms of steric configurations. In systems of high segmental mobility, rich in chain ends, such as DGEBA-DDM (50%), it can be presumed that, for obvious steric hindrance reasons, the segment skeleton configuration is all *trans* (Figure 13a), thus favouring the $I(\text{OH} \dots \text{N})$ bonding. When the segmental mobility decreases, due to crosslinking, more and more segments

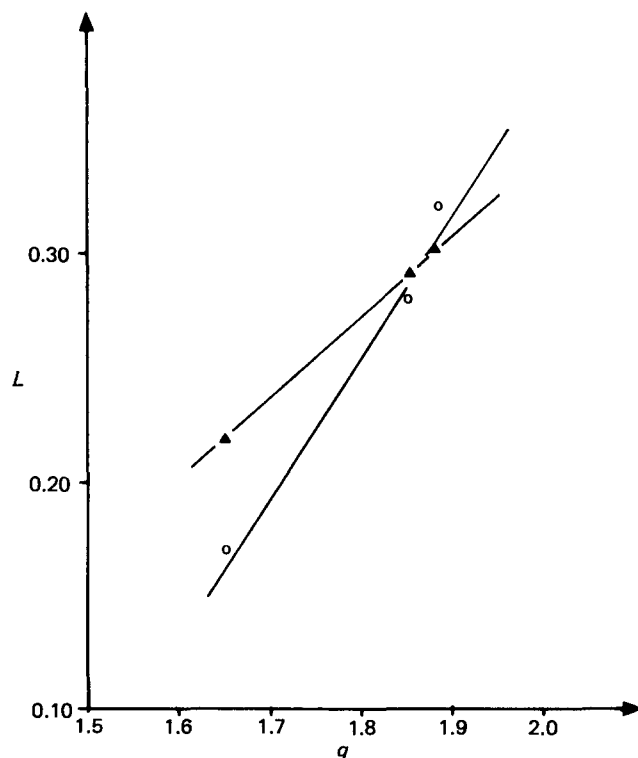


Figure 12 Dependence of L on the electron density q on nitrogen for DGEBA (○) and DGEBF (▲) systems cured with aromatic diamines

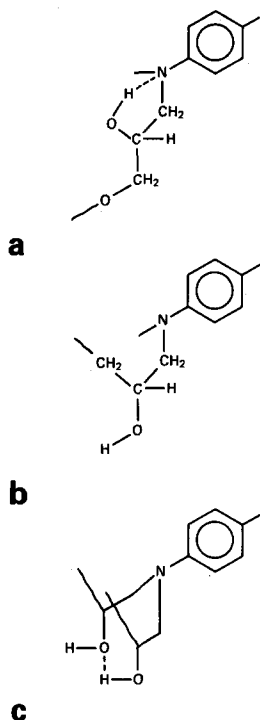


Figure 13 Steric configurations around the sec-alcohol- α -aminomethylene bond: (a) allowing chelate formation; (b) 'folded' segment without $I(\text{OH} \dots \text{N})$ band; (c) hypothetical configuration of the $I(\text{OH} \dots \text{OH})$ species

can be trapped in disfavoured 'folded' configurations, as shown for instance in Figure 13b, in which intrasegmental bonding is forbidden. The intramolecular $I(\text{OH} \dots \text{OH})$ bonding ('H') is favoured at the same time. It can be deduced that it needs the presence of a conformer of higher potential energy than that needed for $I(\text{OH} \dots \text{N})$ bonds. A hypothetical configuration of 'H' is shown in Figure 13c.

Some additional comments can be made:

(a) The relatively low H value for DDS systems (Figure 7) can be explained by the existence, in these systems, of a supplementary H-bonded species, presumably $E(\text{OH} \dots \text{O}-\text{S}-\text{O})$, attested by the presence of three distinguishable components in the hydroxyl band. Further studies on model compounds are needed to assign unequivocally the bands at 3410 and 3460 cm^{-1} .

(b) For a given crosslink density (or T_g value), L is higher for DGEBA-DDM-aniline sample than for DGEBA-DDM ones (Figure 9). This can be explained by the fact that aniline nitrogen is slightly more nucleophilic than nitrogen in DDM¹³.

(c) In the case of alkyl-substituted DDM systems, no relationship is to be expected between L and the amine reactivity in crosslinking owing to the specific influence of

the steric hindrance in the latter. Their high L values reflect the inductive effects of *o*-alkyl groups on the nitrogen nucleophilicity, but could also be affected by other structural parameters. Configurational changes linked to rotations in the immediate vicinity of nitrogen are for instance strongly hindered. This consideration, which needs further investigation, can explain the fact that these systems constitute a peculiar family as shown in Figure 7.

CONCLUSIONS

The influence of structure on the shape of stretching hydroxyl i.r. band of epoxide-amine networks is well explained by the existence of at least three hydrogen-bonded species, $I(\text{OH} \dots \text{N})$, $I(\text{OH} \dots \text{OH})$ and $E(\text{OH} \dots \text{OH})$, whose importance depends mainly on amine nucleophilicity and segmental mobility. Quantitative measurements at various wavenumbers in the 3600–3200 cm^{-1} spectral range or spectral deconvolution could offer in the future interesting prospects for the study of steric configurations or the interpretation of some physical properties presumably dependent on hydrogen bonding, for instance elastic modulus in the glassy state, packing density and water absorption.

ACKNOWLEDGEMENT

This work was partially supported by the 'Direction des Recherches, Etudes et Techniques' which is gratefully acknowledged.

REFERENCES

- 1 Pimentel, G. C. and McClellan, A. L. 'The Hydrogen Bond', Freeman, London, 1960
- 2 Lee, H. and Neville, K. 'Handbook of Epoxy Resins', McGraw-Hill, New York, 1982, p. 4
- 3 Vladimirov, L. V., Zelenetskii, A. N. and Oleinik, E. F. *Vysokomol. Soyed* 1977, **A19**, 2104
- 4 Bellenger, V., Morel, E. and Verdu, J. *Polymer* 1985, **26**, 1719
- 5 Harrod, H. J. *J. Polym. Sci.* 1963, **A1**, 385
- 6 Noskov, A. M. *Zh. Prikladnoi Spektrosk.* 1975, **22** (2), 246
- 7 Bellenger, V. and Verdu, J. *J. Appl. Polym. Sci.* 1985, **30**, 363
- 8 Coggeshall, N. D. and Saier, E. L. *J. Am. Chem. Soc.* 1951, **73**, 5414
- 9 Huggins, C. M. and Pimentel, G. C. *J. Phys. Chem.* 1956, **60**, 1645
- 10 Nakamoto, K., Margoshes, M. and Rundle, R. E. *J. Am. Chem. Soc.* 1955, **77**, 6480
- 11 Cross, A. D. 'Practical Infrared Spectroscopy', Butterworths, London, (French transl. Azoulay, Paris, 1967)
- 12 Eichler, V. J. and Mleziva, J. *Angew. Makromol. Chem.* 1971, **19**, 31
- 13 Diamant, Y., Marom, G. and Broutman, L. J. *J. Appl. Polym. Sci.* 1981, **26**, 3015